

VERIFICATION OF MERIS LEVEL 2 PRODUCTS: CLOUD TOP PRESSURE AND CLOUD OPTICAL THICKNESS

Rene Preusker⁽¹⁾, Peter Albert⁽²⁾ and Juergen Fischer⁽³⁾

17th December 2002

*Freie Universitaet Berlin
Institut fuer Weltraumwissenschaften
Carl-Heinrich-Becker-Weg 6-10
D-12165 Berlin
Germany*

⁽¹⁾ *Email : rene.preusker@wew.fu-berlin.de*

⁽²⁾ *Email : peter.albert@wew.fu-berlin.de*

⁽³⁾ *Email : fischer@zedat.fu-berlin.de*

1 INTRODUCTION

For the verification of the MERIS cloud products, a number of images above several sites above western Europe has been analyzed. The verification of the cloud products consists of three independent methods. The most important task during the verification phase was a manual review to find artefacts and non-physical values. Additionally a comparison with cloud top pressures estimated from radiosonde data and a comparison with cloud top pressures from NASA's MODIS MOD06 product have been made. The data which has been studied is summarized in Tab. 1 and is obtainable at [1].

2 MERIS CLOUD OPTICAL THICKNESS

The cloud optical thickness is estimated from measurements of MERIS channel 10 at 753.75nm. To account for the non-isotropical reflection and transmission properties of clouds the results of radiative transfer simulations have been inverted using polynomials of the third order. The polynomial coefficients are stored in look up tables at discrete angles of viewing and sun geometry determined by the radiative transfer code. The processor also considers the surface albedo, if known. It is used for a pre-selection of the appropriate coefficients which are then interpolated to the actual observation and sun geometry of a pixel. The algorithm is described in more detail in the ATBD [6].

3 MERIS CLOUD TOP PRESSURE

For the retrieval of the cloud top pressure the algorithm uses reflected solar radiation within the oxygen A band absorption centered at 0.76 μ m. It is based on the assumption that the mean photon path length of the reflected solar radiation is related to the amount of absorption measured in the O2A band. In a cloudy atmosphere the mean photon path length is

primary determined by the air mass above the cloud, the cloud top pressure. Hence the cloud top pressure can be estimated through the ratio of measured radiance in an absorption and a window channel. However multiple scattering of photons within the clouds and between the clouds and the surface significantly increase the photon path and must therefore be considered. This is done by the inversion of radiative transfer calculations using artificial neural networks. The algorithm is described in more detail in the ATBD [5]. It has been found that the algorithm is very sensitive to the center wavelength of the absorbing channel. To account for this and to the fact, that the center wavelengths of all channels are different for all pixel, 31 identical neural networks have been trained according to 31 different positions of the central wavelength of channel 11 between 759.0nm and 762.0nm. Within the processing the proper net is chosen according to a spectral shift index which describes the deviation of the pixel channel from the nominal position. The spectral shifts of each pixel have been determined during a spectral calibration campaign in spring 2002.

4 VERIFICATION BY MANUAL REVIEW

Since clouds are very variable in time and space there are only a few rules that can be used for a manual review:

1. Clouds can not be lower than surface pressure and higher than 200-150 hPa.
2. Clouds can not have a negative optical thickness
3. Cloud top height and optical thickness must be independent from all instrumental properties (viewing zenith, azimuth angle, module number and other)

Thus a manual review can only find very basic errors in the processing and not validate the quantities. The cloud optical thickness shows no artefacts and no exceeding of physical limits. The cloud top pressure had some visible artefacts. A first look at the MERIS cloud top pressure product shows a clear striping belonging to the spectral shift index of the pixel and to the different modules (Fig. 1 left). The reason for the discontinuities between the camera modules was a incorrect implementation of the spectral shift index. After a correction there were still small discontinuities belonging to the spectral shift index (Fig. 1 middle). This was not surprisingly since the spectral shift index itself is discontinuous. However the magnitude of the jumps were smaller than the expected accuracy of the cloud top pressure product. To test whether discontinuities vanish when a continuous value for the central wavelength of the absorption channel is used instead of an index, a new breadboard has been developed. The right side of Fig.1 is the same MERIS scene as on the left side, but processed with the new breadboard. The central wavelength of the absorption channel has been taken from the spectral calibration campaign of April 2002. It shows no striping. In the overlap region between the different MERIS modules the assignment of the pixel to the camera and therewith to the results of the spectral calibration is not unique and out of the scope of the breadboard. These pixel have not been processed and they occur as stripes in all images. The new version of the cloud top pressure processor will be implemented in the MERIS ground segment by a software update in Jan 2003. All results presented in the following sections are based on the newest breadboard.

Clouds are very variable atmospheric objects, however in some regions the probability for low and thin stratocumulus clouds is significantly higher. One of these regions is the Atlantic ocean around the Canary Islands. In Fig. 2 the optical thickness and the cloud top pressure from one scene above the Canary Island is shown. The optical thickness is in the order of 10 for most of the clouds and the clouds are lower than 800 hPa. These values correspond well to the expected values.

Summarizing this section, the manual review of the MERIS cloud products was successful. The products show no artefacts using the new breadboard, all values are within the physical range and the cloud top pressure in the west Atlantic passat area are as expected.

5 VERIFICATION USING RADIOSONDES

The profile of relative humidity and temperature from radiosonde data can give some information about the probability of clouds. Finally all radio sounding based cloud detection methods use the fact that the relative humidity within clouds is about 100%. But the relative humidity measured by radiosondes is systematically underestimated especially when the radiosonde passes a cloud. Some attempts have been made to overcome this problem [3, 4], by using the second derivative of relative humidity and temperature as a measure for a local maximum and a temperature dependent threshold of relative humidity for the cloud detection. Considering the limitations of radiosonde data, only simple cases have been selected for a comparison. Simple means here that the profile of relative humidity should allow us a unique determination of the cloud top. For all test cases 57 radiosonde data sets have been found in an archive at the University of Wyoming [2] that are within a cloudy area and show a strong decrease from a high degree of relative humidity.

Most of the radiosonde data is from 12:00 UTC, some datasets are from 6:00 UTC if no 12:00 UTC data is available. Fig. 3 shows two examples of radiosonde data and MERIS cloud top pressure in a 0.5° square around the launch point of the sonde. Fig. 4 shows the scatter diagram of all retrieved cloud heights. The error-bars for the radiosonde data were set to 50 hPa. The median cloud top in the 0.5° square around the radiosonde launch point was taken as the MERIS cloud top height, the twofold standard deviation within this area as the error-bar for the MERIS data. The overall agreement between both methods is good. The standard deviation is in the order of 70hPa. A small bias of -20hPa may point to an over estimation of the MERIS cloud top pressure but actually the accuracy of the radiosonde cloud top height and the time correlation between the launch and the over-paths is too low for this statement. However the verification of the MERIS cloud top pressure was successful since all data is within the individual error limits and no outliers have been found.

6 VERIFICATION USING MODIS MOD06 CLOUD TOP HEIGHTS

The Moderate Resolution Imaging Spectroradiometer MODIS on TERRA allows the retrieval of cloud top pressure using measurements in the thermal infrared between $10\mu\text{m}$ and $14\mu\text{m}$. The most prominent method for this is the CO_2 -slicing [8]. Cloud top heights retrieved from MODIS data using the CO_2 -slicing are part of the MOD06 product, which is available to the public. A detailed description of this product can be found in the ATBD [9]. However the MODIS cloud top height has only a limited accuracy of about 50-150 hPa[7].

The goal of the comparison of MERIS and MODIS cloud top pressures was to find and identify regions or situations where the MERIS processor produces incorrect results. The comparison is limited by two important reasons. Firstly, although the satellites TERRA and ENVISAT are on sun synchronous descending orbits with a crossing time of about 10:30 there is no exact co-location between them. For each MERIS scene a MODIS scene 70 minutes later is available. In many cases a scene 30 minutes earlier is available also. Secondly, both methods belong to different physical principles. MODIS is using thermal infrared channels and is therefore very sensitive for high cold clouds. Thin cold cirrus clouds above thick low-level clouds are almost invisible for MERIS but they are visible with the thermal channels of MODIS.

All co-located MODIS and MERIS scenes have been mapped onto a common regular longitude-latitude grid, using nearest neighborhood sampling. Fig. 5 shows an example of both remapped cloud top heights and a two dimensional histogram of co-appearing cloud top heights, where red means a high number, blue a low number of cases. In this case the time difference between both over-paths is very small. Thus the time difference can not explain the differences for the high clouds in the south west of the area. The low level clouds in the south east of the area agree quite well. The tendency of MODIS towards higher clouds has been observed for several cases. Fig. 6 shows the scatter diagram of all median cloud top heights of all scenes. The error-bars are the standard deviations of the cloud top pressures within one scene. The overall agreement is good, but as seen in the above mentioned example MODIS shows a tendency towards higher clouds. This tendency increases for high level clouds which can be seen in Fig 6. Here the difference between cloud top pressures of MERIS and MODIS is shown as a function of the cloud top pressure of MODIS (the color coding is like in Fig. 5). For low level clouds the bias between both satellites is in the order of -50hPa, for high level clouds the bias increases to 150 hPa.

These differences need further and deeper investigations using additional independent data sources like cloud radars. Nevertheless, no cases have been found where the differences between MODIS and MERIS exceed their accuracy.

7 SUMMARY

The verification of the MERIS cloud products was successful. The cloud top pressure and the cloud optical thickness show no artefacts and non-physical values. All values were within the expected range. The cloud top pressure has been verified additionally using radiosonde data and MODIS cloud top pressure data. Both verification efforts were successful. All retrieved cloud top pressures were within the accuracy limits. However, MERIS has the tendency to retrieve higher cloud top pressures than MODIS. This has to be examined in more detail, within a real validation experiment using additional data sources like ground based cloud RADAR aircrafts.

REFERENCES

- [1] <http://wew.met.fu-berlin.de/meris>.
- [2] <http://weather.uwyo.edu/upperair/sounding.html>.
- [3] E. Arabey. Radiosonde data as means of revealing cloud layers. *Meteor. Gidrol.*, 6:32–37, 1975.
- [4] I. Chernykh and R. Eskridge. Determination of cloud amount and level from radiosonde soundings. *Journal of Applied Meteorology*, 35:1362–1369, 1996.
- [5] J. Fischer, R. Preusker, and L. Schüller. ATBD cloud top pressure. Algorithm Theoretical Basis Document PO-TN-MEL-GS-0006, European Space Agency, 1997.
- [6] J. Fischer, L. Schüller, and R. Preusker. ATBD cloud albedo and cloud optical thickness. Algorithm Theoretical Basis Document PO-TN-MEL-GS-0005, European Space Agency, 1997.
- [7] R. A. Frey, B. A. Baum, W. P. Menzel, S. A. Ackerman, and C. C. Moeller. A comparison of cloud top heights computed from airborne lidar and mas radiance data using CO₂-slicing. *J. Geophys. Res.*, 104:24547–24555, 1999.
- [8] D. J. McCleese and L. S. Wilson. Cloud top height from temperature sounding instruments. *Quart. J. R. Met. Soc.*, 102:781–790, 1976.
- [9] P. Menzel and K Strabala. ATBD cloud top properties and cloud phase. Algorithm Theoretical Basis Document ATBD-MOD-04, NASA, 2002.

TABLES

Table 1: Date and time (in UTC) of all MERIS and MODIS scenes. The last column gives the identification numbers of the radiosonde station that have been used for verification of cloud top pressure.

Location	MERIS date and time	MODIS times	co-located usable RS stations
South Baltic	10/12 9:27	10:38	6181
	10/18 9:39	10:02	6181,10468
	10/21 9:45	8:53, 10:32	6181,10468,10393
	10/24 9:51	9:24, 11:03	-
Lake Constance	10/18 9:39	10:02	14240,10410
	10/21 9:45	8:53, 10:32	7481,16245,16080,16144
	10/24 9:51	9:24, 11:03	7761,16245,16080,14240,10468
Bordeaux	10/13 10:36	11:21	7145
	10/16 10:42	10:14, 11:52	7510,7145
	10/20 10:23	9:49, 11:28	7510,7145
	11/8 10:22	10:20	-
Cabau (NL)	10/17 10:11	9:18, 10:57	6447,7145,11520,10393
	10/20 10:17	9:49, 11:28	6181,6447
	11/08 10:22	10:20	10410
Chilbolton (GB)	10/13 10:36	9:43, 11:21	7145
	10/16 10:42	10:14, 11:52	7145,10410
	10/19 10:48	10:45	7145,6447,3808
Geesthacht (D)	10/17 10:11	09:18, 10:57	6447,7145,10393,10468,11520
	10/20 10:17	09:49, 11:28	6181
	10/21 9:45	8:53, 10:32	-
	10/24 9:51	9:24, 11:03	10468
Canary Islands	10/12 11:17	10:38, 12:16	8552
	10/21 11:26	12:10	8552
Lindenberg (D)	10/12 9:27	10:38	6181,16044,14240,11520
	10/18 9:39	10:02	16044
	10/21 9:45	8:53, 10:32	6474,10410
	10/24 9:51	9:24, 11:03	-
North Sea	10/13 10:36	9:43, 11:21	-
	10/16 10:42	10:14, 11:52	7145
	10/20 10:17	9:49, 11:28	6447
	10/23 10:23	-	7145, 7481,10468,10410
	11/08 10:22	10:20	-

FIGURES

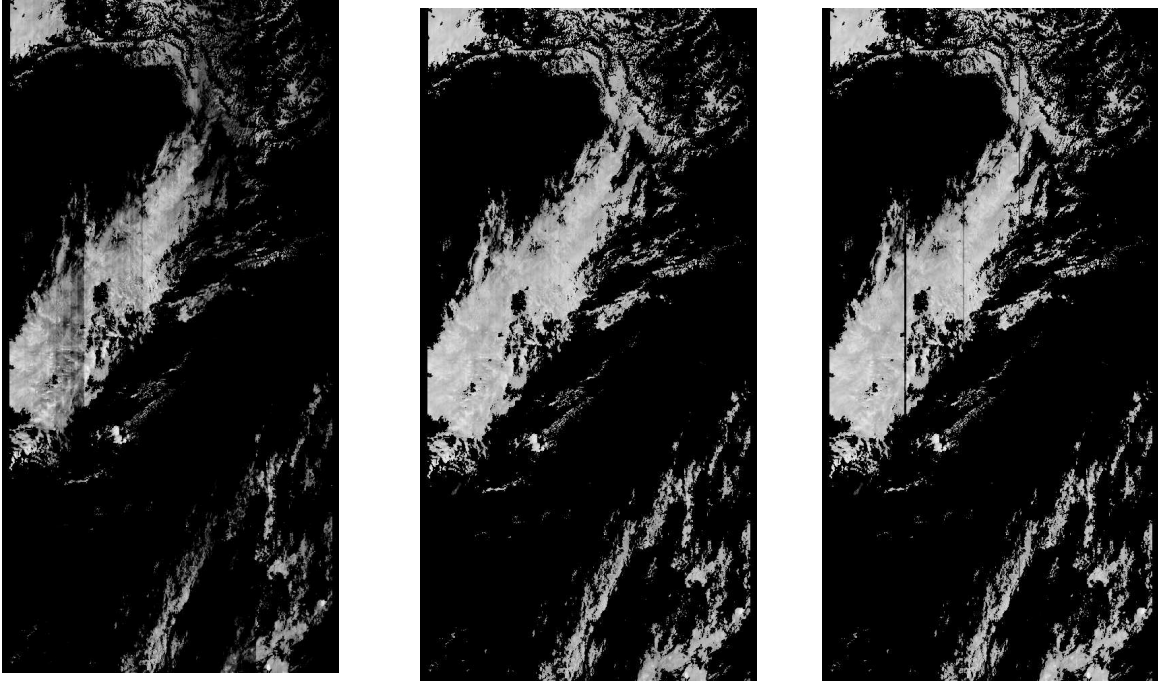


Figure 1: Cloud top pressure estimated with the original MERIS processor (left), with original MERIS processor but corrected spectral shift index (middle) and with the new breadboard(right).

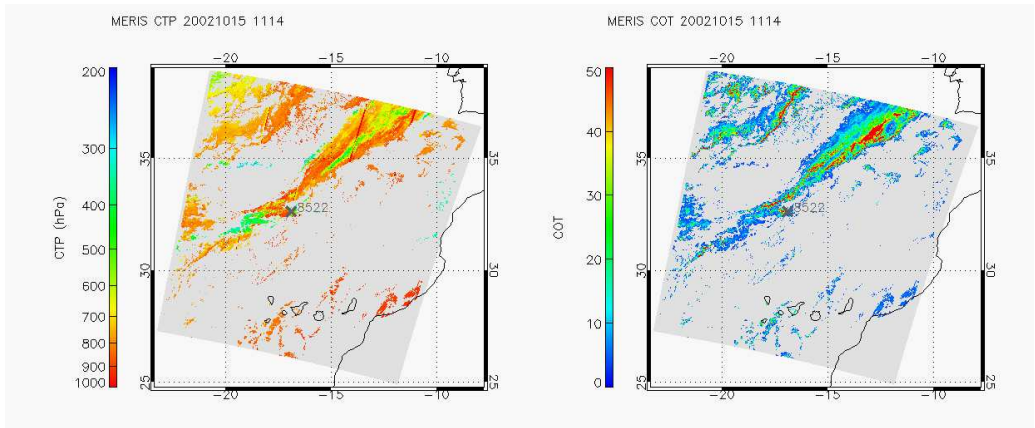


Figure 2: Cloud top pressure (left) and cloud optical thickness(right) for the west Atlantic including the area around the canary islands.

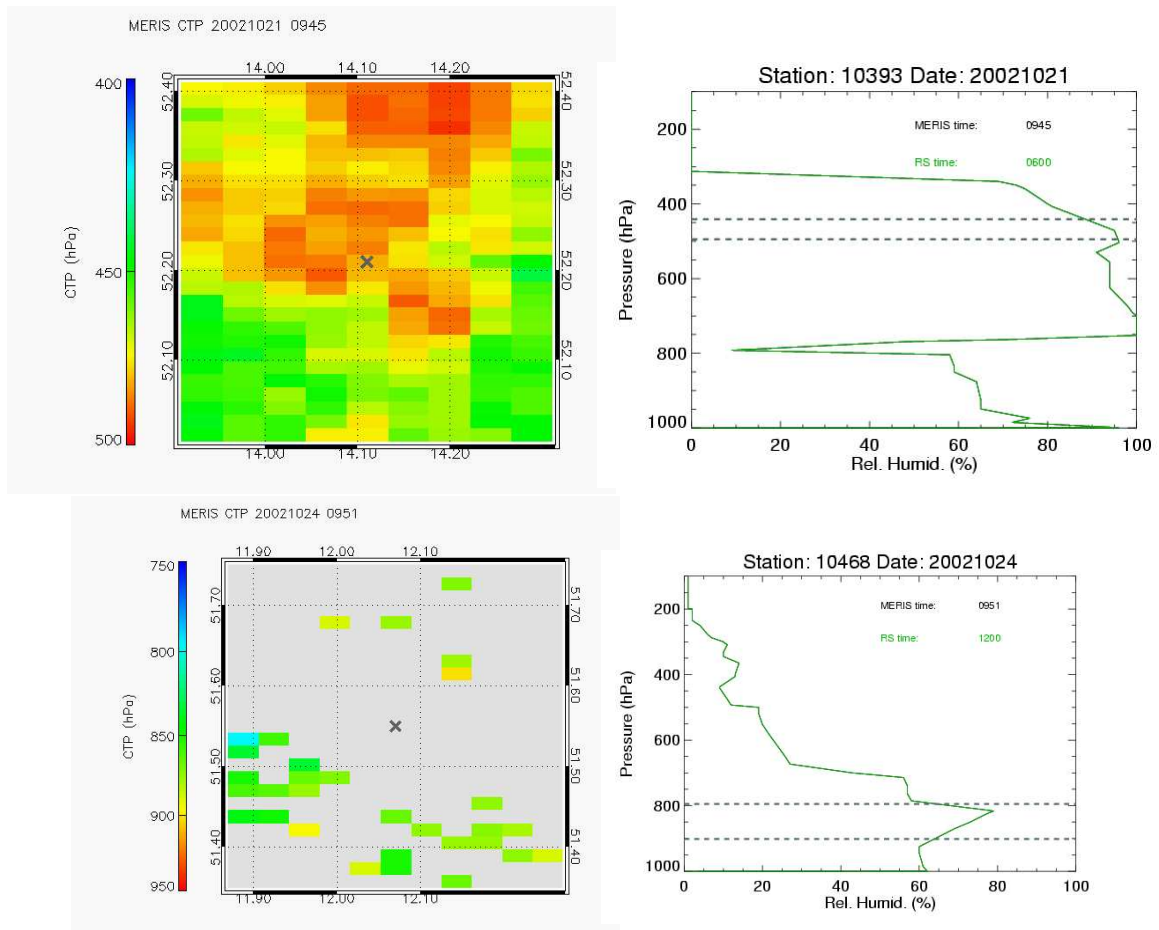


Figure 3: Example of the retrieved MERIS cloud top pressure and relative humidity profile for a high level cloud (upper) and a low level cloud(lower).

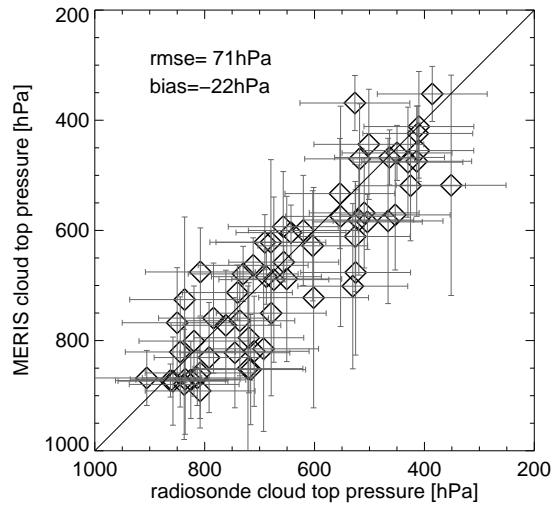


Figure 4: Scatterplot of all used radiosonde data and the corresponding MERIS cloud top pressure.

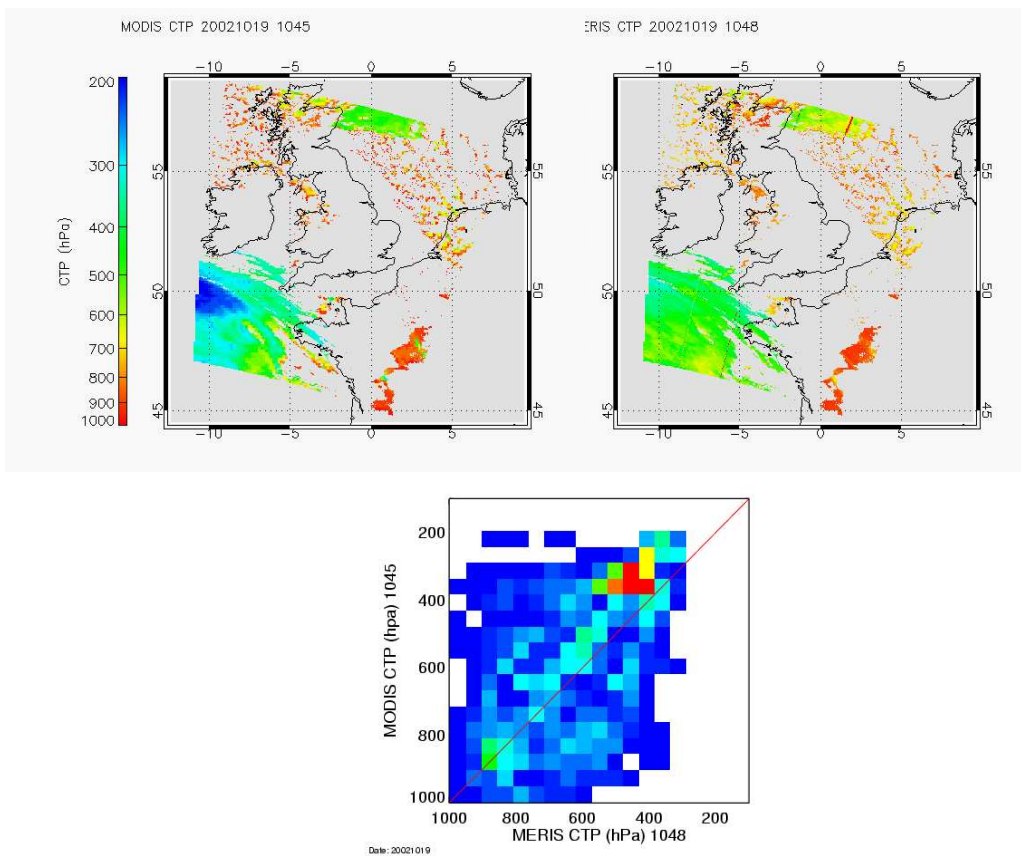


Figure 5: Example for MERIS(right) and MODIS(left) co-located cloud top pressure data. The lower image shows the distribution of co-located cloud top pressures (red: high number, blue: low number)

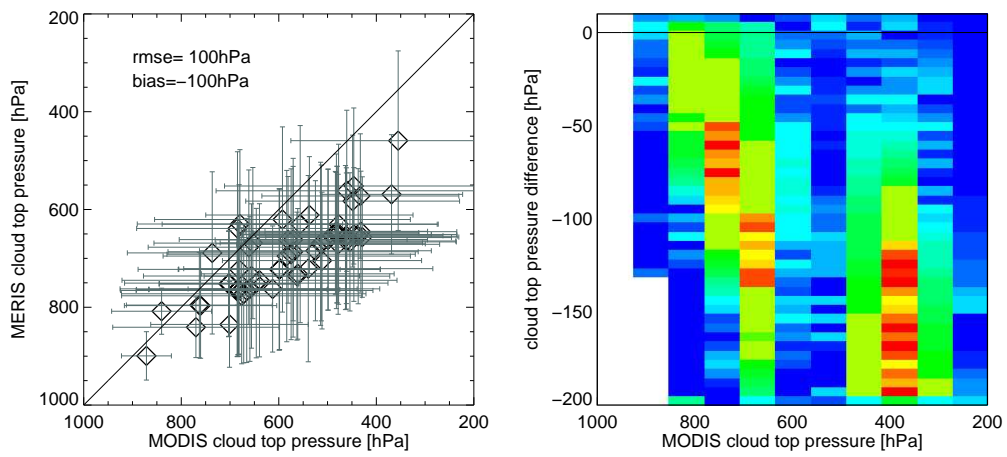


Figure 6: The left diagram shows a scatter plot between the median MODIS and the median MERIS cloud top pressures for all considered scenes. The error-bars are the standard deviations of each scene. The right image shows the distribution of the difference between the co-located MERIS and MODIS cloud top pressure as a function of MODIS' cloud top pressure.